Antiferromagnetic Resonance in MnF_2†

FRED M. JOHNSON* AND ARTHUR H. NETHERCOT, JR.‡
Columbia Radiation Laboratory, Columbia University, New York, New York
(Received November 25, 1958)

Measurements of the antiferromagnetic resonance frequency, $\nu(T)$, were made on single-crystal slabs of MnF_2 in the frequency range 96 to 247.2 kMc/sec and at temperatures, T, ranging from 4.2°K to 64°K ($T_N=67.7$°K). The results are in general agreement with the resonance relations derived for antiferromagnetic materials by Nagamiya, Keffer, and Kittel, and others. At low temperatures, values of $\nu(T)/\nu(0)$ and $\nu(0)$ are consistent with spin-wave method calculations of the sublattice magnetization and of the value and temperature dependence of the anisotropy energy. This agreement indicates almost complete correlation of adjacent electron spins in the low-temperature range as predicted from spin-wave theory.

From the antiferromagnetic resonance measurement of $\nu(0)=261.4\pm1.5$ kMc/sec and Oguchi's calculation of H_A, $z|J|$ is 3.94×10^{-15} erg, in agreement with other determinations. Antiferromagnetic resonance line widths were measured from 4.2°K to 64°K. The observed asymmetric line shapes are satisfactorily accounted for as arising from a mixing of absorption and dispersion and from reflections. A simplified line-width theory is given which satisfactorily accounts for the observed line widths except at the lowest temperatures, where a residual width is found. Finally, antiferromagnetic resonance measurements on two crystals, which were grown under different conditions, indicate no difference in resonance frequency or line width.

I. INTRODUCTION

THE theoretical and experimental investigation of antiferromagnetic resonance (AFMR) has been of recent origin. The first investigations[1,2] were concerned with the very rapid disappearance of the paramagnetic resonance absorption close to the Néel temperature (T_N). This phenomenon was readily understood following several theoretical papers on antiferromagnetic resonance.[3–8] These papers showed that below the Néel temperature the resonance frequency depends strongly on both the exchange field (H_E) and the anisotropy field (H_A):

$$\nu_{H=0}\simeq(\gamma/2\pi)(2H_EH_A)^{\frac{1}{2}}, \quad \text{if} \quad H_A\ll H_E.$$

Antiferromagnetic materials having a low Néel temperature and hence a small H_E might be expected to have resonance frequencies in the conventional microwave region. $CuCl_2\cdot2H_2O$ ($T_N=4.3$°K) falls in this category and has been extensively investigated by the Leiden group.[9] The interpretations of AFMR experiments on this and on other materials[10] ($CuBr_2\cdot2H_2O$) have been complicated by the elaborate equations necessary if the crystal does not have uniaxial symmetry. Experiments on Cr_2O_3 near T_N have also been reported.[11]

MnF_2, on the other hand, makes possible a very direct and simple test of the basic theory. However, very high frequencies (in the shorter millimeter wave range) or very strong fields (over 30 000 gauss) are necessary in order to observe the resonance in the antiferromagnetic state. The AFMR measurements described in this paper were made at frequencies ranging from 96 kMc/sec to 247.2 kMc/sec. A preliminary report of some of the results has previously been made.[12] Foner[13] has also recently observed, with less precision, AFMR in MnF_2, using pulsed magnetic fields and relatively low frequencies (35 kMc/sec and 70 kMc/sec). The disappearance of the paramagnetic resonance in MnF_2 near 67.7°K (T_N) has been investigated by Hutchison.[14]

The magnetic carriers in MnF_2 are the Mn^{++} ions, whose electrons are essentially in a ${}^6S_{\frac{5}{2}}$ state. The magnetic structure of MnF_2, which has been uniquely determined by neutron diffraction studies,[15] is shown in Fig. 1. The unit cell[16] has tetragonal symmetry and may be conveniently pictured as a body-centered cube compressed along the c axis. The magnetic unit cell has the same dimensions as the chemical unit cell.

At temperatures below T_N, exchange forces establish the antiparallel alignment and anisotropy forces align the spins along the c axis. As a result, the magnetic moments will point predominantly parallel and antiparallel to the c axis. The lower the temperature, the more perfect this alignment will be.

† Work supported jointly by the U. S. Army Signal Corps, the Office of Naval Research, and the Air Force Office of Scientific Research.
* Now at RCA Laboratories, Princeton, New Jersey.
‡ Now at the IBM Watson Scientific Laboratory at Columbia University, New York, New York. A part of the work was performed while at this location.
[1] Trounson, Bleil, Wangsness, and Maxwell, Phys. Rev. **79**, 542 (1950).
[2] L. R. Maxwell and T. R. McGuire, Revs. Modern Phys. **25**, 279 (1953) and references cited therein.
[3] T. Nagamiya, Progr. Theoret. Phys. (Kyoto) **6**, 350 (1951).
[4] C. Kittel, Phys. Rev. **82**, 565 (1951).
[5] F. Keffer and C. Kittel, Phys. Rev. **85**, 329 (1952).
[6] R. K. Wangsness, Phys. Rev. **86**, 146 (1952).
[7] C. J. Gorter and J. Haantjes, Physica **18**, 285 (1952).
[8] F. Brown and D. Park, Phys. Rev. **93**, 381 (1954).
[9] The most complete accounts of these investigations are contained in the thesis of J. Ubbink, 1953 (unpublished), and that of H. J. Gerritsen, 1955 (unpublished). These accounts are largely duplicated, however, in a series of papers starting with that of Poulis, van den Handel, Ubbink, and Gorter, Phys. Rev. **82**, 552 (1951). The paper by H. J. Gerritsen and M. Garber, Physica **22**, 481 (1956), gives later references.
[10] M. Date, Phys. Rev. **104**, 623 (1956).
[11] E. S. Dayhoff, Phys. Rev. **107**, 84 (1957).
[12] F. M. Johnson and A. H. Nethercot, Jr., Phys. Rev. **104**, 847 (1956).
[13] S. Foner, Phys. Rev. **107**, 683 (1957).
[14] C. A. Hutchison (unpublished), quoted by L. R. Maxwell, Am. J. Phys. **20**, 80 (1952).
[15] R. A. Erickson, Phys. Rev. **90**, 779 (1953).
[16] M. Griffel and J. W. Stout, J. Am. Chem. Soc. **72**, 4351 (1950).

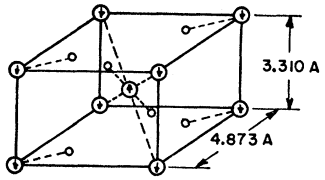

FIG. 1. Magnetic structure of MnF_2. Shown are the order and orientation of the Mn^{++} magnetic moments. The small circles correspond to fluorine sites (after Erickson).

The major reasons for investigating AFMR in MnF_2 are as follows: (1) Its magnetic structure is very similar to that embodied in the two-sublattice model of antiferromagnetism discussed by Van Vleck[17] and others. (2) Detailed calculations by Keffer[18] and Oguchi[19] on the anisotropy field give a theoretical prediction of the value of the resonance frequency and its dependence on temperature. (3) Related experiments on MnF_2 [such as magnetic susceptibility measurements,[20,21] neutron diffraction studies[15] of $M(T)$, and nuclear magnetic resonance studies[22] of the fluorine nuclei] allow a more complete interpretation to be made, especially of the temperature dependence of the sublattice magnetization.

Since the original report,[12] the thermometry has been greatly improved and this has resulted in more precise temperature measurements; also, measurements have been extended into the temperature range from 36°K down to 4°K and into the frequency range up to 247.2 kMc/sec. These experiments have yielded new data on both the line width and on the behavior of the resonance frequency as a function of temperature. These results make possible an experimental check of recent spin-wave calculations on the dependence of the resonance frequency and magnetization on temperature.

II. THEORY

Although the theory of antiferromagnetic resonance was developed by several investigators[3,4] at approximately the same time, we shall follow the notation and method of Keffer and Kittel.[5] This paper shows that, for a uniaxial crystal with the static field parallel to the symmetry axis, the Larmor precession frequency is given by

$$\omega/\gamma=\pm H(1-\tfrac{1}{2}\alpha)+[(2H_E+H_A)H_A+(\tfrac{1}{2}\alpha)^2(H)^2]^{\frac{1}{2}}. \quad (1)$$

Here H_E is the exchange field, H_A is the anisotropy field, H is the externally applied magnetic field, γ is $ge/2mc$ (the magnetomechanical ratio), and α is the ratio of the static susceptibilities measured parallel and perpendicular to the c axis. Since in our experiment H was very small compared to $2H_EH_A$ and H_A small compared to $2H_E$, Eq. (1) can be written as

$$2\pi\nu/\gamma=\omega/\gamma=\pm H(1-\tfrac{1}{2}\alpha)+(2H_EH_A)^{\frac{1}{2}}. \quad (2)$$

α varies from 0 to 1 as the temperature goes from 0° to 67.7°K.

Keffer[11] has estimated H_E and H_A for MnF_2 at 0°K. He calculated the anisotropy field as 8800 gauss, of which 8300 gauss arise from dipole-dipole interactions and 500 gauss from interactions with the crystalline electric field. From molecular field theory,

$$H_E=M_0/\chi_\perp. \quad (3)$$

Also, $M_0/0.97=M_\infty=Ng\beta S=590$ gauss. The measured value[21] of $\chi_\perp$ ($=1.030\times10^{-3}$ per cc) gives an H_E of 556 000 gauss. Therefore $(2H_EH_A)^{\frac{1}{2}}$ is predicted to be 97 500 gauss at 0°K.

In order to obtain the temperature dependence of $(2H_EH_A)^{\frac{1}{2}}$ it was previously[18,12] assumed that $H_A\propto M$. This is the dependence that molecular field theory would predict if there were no local ordering effects. Then

$$\nu_{H=0}=K'M(T)/M(0)=K'B_{\frac{5}{2}}(T/T_N). \quad (4)$$

Here $B_{\frac{5}{2}}(T/T_N)$ is the modified Brillouin function for the spin $\frac{5}{2}$, where the argument $(\mu|H_{\text{eff}}|/kT)$ has been transformed to (T/T_N) through the relationship:

$$y=\mu|H_{\text{eff}}|/kT=\frac{T_N}{T}\frac{B_{\frac{5}{2}}(y)}{(dB/dy)_{T=T_N}}.$$

Values of $B_{\frac{5}{2}}(T/T_N)$ were calculated from the tables of Schmid and Smart.[23]

The original data (at temperatures down to 42°K) fitted expression (4) very well with a value of $K'=264\pm5$ kMc/sec, or $(2H_EH_A)^{\frac{1}{2}}=94\,300\pm4000$ gauss at $T=0$°K. It might be expected that expression (4) would fail at temperatures much lower than 40°K since the spin wave theory would predict a different dependence of M upon T and might also destroy the direct proportionality assumed between H_A and M.

Calculations of $M(T)/M_\infty$ applicable to low temperatures have been made by Anderson,[24] Kubo,[25] and Eisele and Keffer[26] using spin wave theory. For a body-centered lattice, the final expression[26] for the sublattice magnetization, $M(T)$, including a small correction[27] factor 1.025, is

$$M(T)=M_\infty[0.97-(1.025)(4/15)\theta^2M(T/T_{AE})], \quad (5)$$

where

$$M(T/T_{AE})=\left(\frac{6}{\pi^2}\right)\left(\frac{T_{AE}}{T}\right)\sum_{n=1}^{\infty}\frac{1}{n}K_1(nT_{AE}/T), \quad (6)$$

and K_1 is a Hankel function. Other constants are defined as follows:

$$kT_{AE}=h\nu_{H=0}(0), \quad \text{and} \quad \theta=kT/z|J|S, \quad (7)$$

[17] J. H. Van Vleck, J. Chem. Phys. **9**, 85 (1941).
[18] F. Keffer, Phys. Rev. **87**, 608 (1952).
[19] T. Oguchi, Phys. Rev. **111**, 1063 (1958).
[20] J. W. Stout and M. Griffel, J. Chem. Phys. **18**, 1455 (1950).
[21] H. Bizette and B. Tsai, Compt. rend. **238**, 1575 (1954).
[22] V. Jaccarino and R. G. Shulman, Phys. Rev. **107**, 1196 (1957).
[23] L. P. Schmid and J. S. Smart, U. S. Naval Ordnance Laboratory Report NOrdL-3640, 1954 (unpublished).
[24] P. W. Anderson, Phys. Rev. **86**, 694 (1952).
[25] R. Kubo, Phys. Rev. **87**, 568 (1952).
[26] J. A. Eisele and F. Keffer, Phys. Rev. **96**, 929 (1954).
[27] F. Keffer (private communication).

where $S=\frac{5}{2}$, k=Boltzmann's constant, $|J|/2$ is the exchange integral, and z is the number of nearest neighbors. This expression should be used at the lower temperatures. It reduces to the well-known T^2 law if $T \gg T_{AE}(=12.5°\text{K})$.

Oguchi[19] has recently calculated the temperature dependence of the anisotropy energy in MnF_2 by a spin wave method. According to Oguchi, the temperature dependence of the anisotropy energy is given by

$$E_A(T) \propto M(T)^{2.9}. \tag{8}$$

This corresponds to $H_A \propto M^{1.9}$. (The exponent for H_A would be unity from simple molecular field theory neglecting local ordering; it would be 2.0 for complete correlation of spins.[28]) Therefore in the low-temperature range, the precession frequency from (2) is

$$\omega/\gamma = \pm H(1-\tfrac{1}{2}\alpha)+C[M(T)]^{1.45}, \tag{9}$$

where $M(T)$ should be computed from (5). Finally, substituting for $M(T)$ from Eq. (5),

$$\nu = \pm(\gamma/2\pi)H(1-\tfrac{1}{2}\alpha) + K[0.9568 - aT^2M(T/T_{AE})], \tag{10a}$$

where

$$a = (0.396)(k/z|J|S)^2. \tag{10b}$$

It was assumed here that $(1-\epsilon)^{1.45}=1-1.45\epsilon$.

Since a good theoretical estimate of $z|J|$ does not exist, its value must be deduced from experiments. If the experimentally determined values of $H(1-\frac{1}{2}\alpha)$ for a given value of ν are plotted against the corresponding values of $T^2M(T/T_{AE})$, a straight line should be obtained whose slope will determine the multiplicative constant a and hence $z|J|$ from Eq. (10b).

An alternative and somewhat more accurate method exists for obtaining $z|J|$. This involves the AFMR frequency at 0°K, $\nu(0)$. Since[25]

$$H_E = M/\chi_\perp = 2z|J|M/Ng^2\beta^2 \tag{11}$$

and

$$H_A = E_A/M = 4.86\times10^6/M, \tag{12}$$

from Oguchi's analysis, then

$$\nu(0) = 2.80(4z|J|E_A/Ng^2\beta^2)^{\frac{1}{2}} = 4.15\times10^{12}(z|J|)^{\frac{1}{2}}\ \text{Mc/sec}. \tag{13}$$

Here it was assumed that $g=2.00$. The two values of $z|J|$ obtained from this experiment as well as those obtained by other methods will be discussed in Sec. V.

III. EXPERIMENTAL METHODS

A waveguide transmission spectrometer was used in all the measurements rather than the more conventional microwave cavity spectrometer. In this apparatus a plane parallel slab of MnF_2 was placed across the waveguide and, as the external applied magnetic field was swept through resonance, observations were made on the variation of the power transmitted through the slab. The output of a crystal detector then gave the absorption as a function of applied magnetic field. The very strong absorption intensities at these high frequencies (about 92% absorption in a 0.0045-inch thick slab) made it possible to use this simple arrangement.

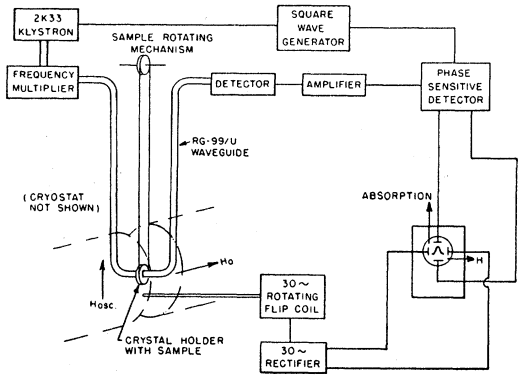

FIG. 2. Experimental arrangement. The block diagram shows the arrangement used for the case of millimeter wave production by crystal harmonic generators.

The advantages of this method are in the broad-band frequency coverage and in the simplicity of the construction. Data were taken at many frequencies from 96 to 247.2 kMc with essentially no changes in the apparatus or in the sample. The major disadvantage of the method is that it is possible to get a distorted line shape because of dispersion and reflections from the faces of the slabs. It was not possible for mechanical reasons to make the slab thin enough to eliminate the problem of reflections.

Two liquid helium cryostats were used during the course of the experiments. It was found that the original cryostat did not transmit power efficiently at the highest frequencies: the transmission varied from about 10% at $\lambda=4$ mm to about $\frac{1}{10}$% at $\lambda=1.2$ mm. The second cryostat was constructed to allow measurements to be made at these highest frequencies. In the original cryostat, the rf power was transmitted to the sample via $a\sim3\frac{1}{2}$-foot length of *RG* 99/*U* wave guide which extended vertically from the top of the cryostat to the bottom of the liquid helium chamber. Following a connecting U-shaped bend, the power transmitted through the sample was then transmitted to the crystal detector via another $3\frac{1}{2}$-foot length of guide. The sample holder was inserted from the top of the cryostat into a $\frac{1}{8}$-inch gap situated at the bottom of the U-shaped bend (see Fig. 2).

Although a number of tests were made, it was impossible to localize and correct the anomalously high transmission loss at $\lambda=1.2$ mm. Therefore it was necessary to alter the design radically in order to improve the performance at 1.2 mm. The second cryostat had fewer bends and only very short connecting lengths of wave

[28] This can readily be seen by extending the classical treatment of Nagamiya, Yosida, and Kubo, *Advances in Physics*, edited by N. F. Mott (Taylor and Francis, Ltd., London, 1955), pp. 71–73.

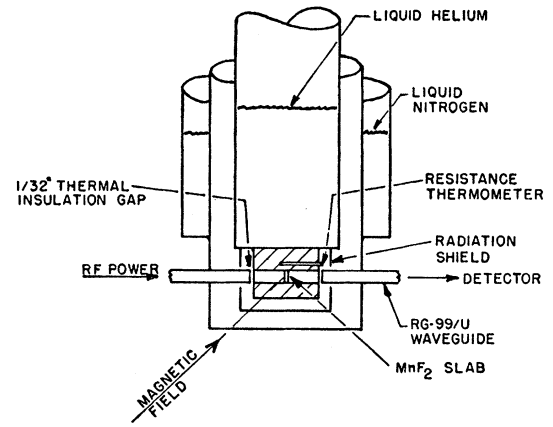

FIG. 3. Schematic diagram of cryostat No. 2.

guide. It provided excellent transmission even at the shortest wavelengths. Figure 3 is a schematic diagram of this design. A one-inch length of *RG* 99/*U* wave guide was hard-soldered into a copper block, which in turn made contact with the liquid helium. The MnF_2 slab was cemented inside this wave guide with coil dope. This guide was separated from the input and output waveguide sections by a vacuum gap of about $\frac{1}{32}$ in. This gap prevented an excessive heat leak along the very short waveg uide. Little loss of microwave power occurred at this gap since the wavelength was quite small compared to the wave guide dimensions. Approximately one half of the microwave power was transmitted through the cryostat at 247.2 kMc/sec.

Since in both cryostats the sample was not immersed in the liquid helium but instead was in contact with metal walls cooled indirectly by the liquid helium, the problem of correctly measuring the temperature of the sample was an important one. Two sample holders were used with the original cryostat. The first was not particularly well designed for accurate temperature measurements, but did permit the sample to be rotated during a run by up to 110° about an axis perpendicular to the dc magnetic field. The temperature was measured by means of a carbon resistance thermometer[29] attached to the copper block $\frac{1}{2}$ inch from the sample. This thermometer was not in the sample holder itself, and temperature gradients could have existed across the simple mechanical contact between the sample holder and the copper block; this could have caused errors in the early temperature measurements. The second holder used a platinum resistance thermometer (Leeds and Northrup No. 8164). This thermometer was not only more reliable and reproducible, but reduced greatly the number of calibration runs necessary. Also, it was placed so that it was in direct contact with the sample holder and not in contact with any other parts of the cryostat. This design ensured very accurate measurements of the temperature of the sample, since it eliminated the possibility of heat conduction causing temperature gradients between the sample and the thermometer. The only errors that could have occurred would have been a direct power input to the sample itself by microwave or infrared radiation. Such errors should be small. The results reported previously[12] were taken with the first sample holder. Many of these measurements were repeated with the platinum thermometer in order to be certain that no systematic errors had been present before. It was found that in fact the two sample holders gave consistent results. The maximum temperature deviation observed between the two thermometers was about 0.3°K. A limitation of the second sample holder was the fact that it could not be rotated.

In the second cryostat, which was designed only for very low temperatures, the platinum thermometer could not be used. A $\frac{1}{10}$-watt, 56-ohm carbon resistor was cemented with glyptal into the copper block (into which the wave-guide section containing the sample was soldered). The sample and thermometer were in close proximity. Heat radiation from the nitrogen bath was minimized by a copper radiation shield attached to the liquid helium can. It was noted that at 4°K there was a temperature gradient between the bath and the thermometer of ~1°K. Probably the major part of this gradient was caused by heat influx along the wires connecting the resistance thermometer. At these low temperatures, the thermal conductivity of the thermometer and its cement is very poor; but as the temperature becomes higher, the gradient rapidly becomes less. This gradient was responsible for the large errors stated in the measurements at the lowest temperatures (±0.6°K), but fortunately the resonance frequency becomes quite insensitive to temperature at very low temperatures.

All these thermometers were calibrated from vapor pressure measurements on liquid nitrogen, oxygen, hydrogen, and helium. Highly purified nitrogen was liquefied for this purpose. The triple point and normal boiling point of liquid nitrogen were given the most weight, but measurements were also made at intermediate temperatures (63°K to 77°K). It was found that temperature differences up to 0.3°K occurred between commercially liquefied nitrogen and that used here. The liquid hydrogen was about 99% equilibrium hydrogen and measurements were taken from 13.8°K to 20.4°K. The tables of Linder[30] were used to convert vapor pressure to temperature. The possible effects (~0 to 0.2°K) of the unknown pressure head in the liquid are included in the stated error. All resistance measurements were made at low currents (10^{-4} amp) with a sensitive dc potentiometer and galvanometer. Resistances were measured to one part in 1000 and relative temperature changes could be read to 10 millidegrees with the platinum resistance thermometer. The various sources of error limited the accuracy of

[29] J. R. Clement and E. H. Quinnell, Rev. Sci. Instr. **23**, 213 (1952).

[30] C. T. Linder, Westinghouse Research Laboratories Report R-94433-2-A, 1950 (unpublished).

temperature determinations variously from ~1° at 4°K to 0.1° at 66°K. Measurements were often taken while the cryostat was warming up with no refrigerating liquid present. By making similar measurements at different rates of warming and also of cooling, it was established that any relative temperature lags of the resistor and sample must be less than 0.1°K.

The strength of the applied magnetic field at the position of the sample was determined by a rotating flip coil[31] which had been calibrated against the proton resonance frequency. The magnetic field measurements were actually made outside of the cryostat, but this field is expected to be equal to that at the sample since the field was quite homogeneous and no magnetic materials were employed in the construction of the cryostat. The flip coil arrangement had a second coil rotating in the fixed reference field of a permanent magnet and measurements were made relative to this magnetic field. The accuracy of the field measurements was determined primarily by the width of the AFMR resonance line.

Microwave power at the lower frequencies (96, 117, and 146 kMc/sec) was produced by crystal harmonic generators driven by 2*K*33 klystrons.[32] Figure 2 gives a block diagram of the experimental arrangement. At the higher frequencies it was more convenient to use the harmonics[32] from millimeter magnetrons.[33] Magnetrons having fundamental wavelengths from 4.0 to 4.8 mm were used and signal-to-noise ratios of 10^6, 10^4 and 10^2, respectively, were obtained at frequencies of 150, 212.7, and 247.2 kMc/sec. A signal-to-noise ratio of 10^6 corresponds to approximately 0.5 watt peak power or 0.1 milliwatt average power.

The frequency of the fundamental of the klystron or magnetron was measured by a calibrated wavemeter. Care was taken to verify by other methods that the harmonic was correctly identified. The final uncertainty of frequency measurements in the 200-kMc region was about ±0.3 kMc/sec.

Crystal Alignment

All the slabs used in this experiment were cut from single crystals of MnF_2. With the exception of two special cases discussed in Sec. VII, they were cut into rectangular shape with the symmetry axis, *c*, in the plane of the slabs and parallel to their short sides. When a crystal slab was in place in the apparatus, the *c* axis was parallel to the applied dc magnetic field and the oscillating magnetic field was perpendicular to the dc field. This particular choice of crystal orientation enabled results to be readily compared with theory.

The sample alignment was checked by a polarizing microscope set for crossed polaroids and also by x-ray Laue diffraction patterns.[34] The accuracy of the alignments with respect to the dc field was about 1° as measured with x-rays and about 2° to 3° with the polarizing microscope. Additional errors possible in the alignment of the crystal with respect to the external magnetic field might have arisen from misalignments of the slab in the waveguide (~2°), and of the crystal holder with respect to magnetic field (~2°). It is estimated that the total error in crystal alignment, from all causes, is about 3°. Errors of this magnitude cannot result in any observable frequency shift of the AFMR at fields below 8000 gauss, a fact which was verified experimentally by rotating the magnet. It was found that a magnet rotation of 5 degrees did not cause an observable effect on the resonance frequency.

IV. LINE SHAPE AND PROPAGATION

For most of the measurements, the MnF_2 slab was placed across the wave guide. As was mentioned previously, the dispersion and consequent reflection associated with this arrangement would tend to distort the line shape. A further distortion occurs because the susceptibility becomes very large. This leads to a mixing of absorption and dispersion and results in a very asymmetric absorption line. These two aforementioned effects seem to explain semiquantitatively the experimental line shapes.

Since both ferromagnetic and antiferromagnetic media are special cases of a more general system of two interpenetrating sublattices,[6] it is expected that microwave transmission through the two types of gyromagnetic medium will have similar properties. This is readily seen by noting that the rf permeability tensor, T_{ij}, for the antiferromagnetic case is similar in form to that for the ferromagnetic case, although, of course, the elements of the tensor are different, *viz.*:

$$T_{ij}=\begin{pmatrix}\mu & -i\kappa & 0\\ i\kappa & \mu & 0\\ 0 & 0 & 1\end{pmatrix}. \tag{14}$$

The tensor elements for the case of cubic symmetry can be inferred from the paper by Keffer and Kittel[5] for 0°K and for arbitrary temperatures by Dayhoff.[35]

At 0°K and for no damping, the elements are

$$\mu=1+2\pi\gamma(2H_EH_A)^{\frac{1}{2}}\chi_1\left\{\frac{\omega_2}{\omega^2-\omega_2^2}+\frac{\omega_3}{\omega^2-\omega_3^2}\right\}, \tag{15}$$

$$\kappa=2\pi\gamma(2H_EH_A)^{\frac{1}{2}}\chi_1\left\{\frac{\omega}{\omega^2-\omega_3^2}-\frac{\omega}{\omega^2-\omega_2^2}\right\}. \tag{16}$$

Here ω_2 and ω_3 are the resonance frequencies,

$$\omega_{2,3}=\pm|\gamma|H+|\gamma|(2H_AH_E)^{\frac{1}{2}}. \tag{17}$$

[31] Dayhoff, Triebwasser, and Lamb, Phys. Rev. **89**, 106 (1953).
[32] See, for example, A. H. Nethercot, Jr., Trans. I.R.E. **MTT2**, 17 (1954).
[33] M. J. Bernstein and N. M. Kroll, Trans. I.R.E. **MTT2**, 33 (1954).
[34] We are indebted to Professor P. F. Kerr for help with the crystal alignment.
[35] E. S. Dayhoff, J. Appl. Phys. **29**, 344 (1958).

For the case of $\omega_2 \neq \omega_3$ and $\omega \simeq \omega_3$, these expressions can be simplified to

$$\mu = 1 + A/(\omega - \omega_3), \qquad \kappa = -A/(\omega - \omega_3), \tag{18}$$

where

$$A = \pi\gamma(2H_E H_A)^{\frac{1}{2}}\chi_\perp. \tag{19}$$

For the case of microwave propagation in a direction perpendicular to the direction of the effective magnetic fields acting on the precessing electrons, the propagation constant is given by[36,37]

$$\Gamma = \frac{i\omega}{c}\epsilon^{\frac{1}{2}}\left(\frac{\mu^2-\kappa^2}{\mu}\right)^{\frac{1}{2}} = \frac{i\omega}{c}\epsilon^{\frac{1}{2}}(\mu_{\text{eff}})^{\frac{1}{2}}, \tag{20}$$

where ϵ is the dielectric constant and is assumed real (this assumption has been verified experimentally).

Introducing a small amount of damping by letting $\omega = \omega + i\delta$, and letting

$$\mu_{\text{eff}} = \mu_1 - i\mu_2, \tag{21}$$

$$\mu_1 = 1 + \frac{x_1 A/\delta}{1+x_1^2}, \quad \mu_2 = \frac{A/\delta}{1+x_1^2}. \tag{22}$$

Here $x_1 = (\omega - \omega_3')/\delta$, $\omega_3' = \omega_3 - A$, and $2\delta = \Delta\nu$ is equal to the full width at half intensity of μ_2. The value of A can be estimated from Eq. (19) and is about 320 gauss at 0°K. If we let $\Gamma = \Gamma_1 - i\Gamma_2$, then we find

$$\Gamma_{1,2} = (i\omega/c)(\epsilon/2)^{\frac{1}{2}}[(\mu_1^2+\mu_2^2)^{\frac{1}{2}} \pm \mu_1]^{\frac{1}{2}}. \tag{23}$$

The power transmitted through the sample is primarily dependent on Γ_2. Neglecting reflections,

$$P/P_0 = e^{-(4\pi/\lambda)\,l\Gamma_2}, \tag{24}$$

where l is the slab thickness ($\sim$0.0045 in.) and P_0 the power transmitted at frequencies far off resonance.

From Eq. (23) and Eq. (24) it can be shown that the transmission drops off much faster on the high-frequency side of the resonance line than on the low-frequency side. This type of asymmetric line shape has been experimentally verified for both the resonance frequencies ω_2 and ω_3.

The total reflection is best analyzed separately in two regions: near the resonance peak where the absorption is large and multiple reflections effectively damped out, and at the wings where constructive and destructive interference is possible. Thus, near the peak,

$$P/P_0 = [(1-R)/(1-R_0)]^2 e^{-(4\pi/\lambda)\,l\Gamma_2}, \tag{25}$$

where R and R_0 are the reflection coefficients at resonance and off-resonance, respectively. At the wings, the effective wavelength inside the slab can be such that the reflections cancel when $2\Gamma_1 l/\lambda = 1$. Numerical evaluation shows that on the high-frequency side of the line, Γ_1 can be large enough for this to occur, but not on the low-frequency side. Therefore P/P_0 may be greater than unity on the high-frequency side of resonance.

[36] C. L. Hogan, Revs. Modern Phys. **25**, 253 (1953).
[37] C. L. Hogan, Proc. Inst. Radio Engrs. 44, 1345 (1956).

V. RESULTS

Measurements of the resonance frequency and line width have been made over the temperature range 4.2 to 64°K. This covers almost the complete antiferromagnetic region ($T_N = 67.7$°K). Measurements have been made both with $H=0$ and $H \neq 0$. The results obtained at $H=0$ are given in Table I. The stated uncertainties in the temperature are primarily due to the difficulty in determining the center of the line due to its large line width.

Measurements of ν made with $H \neq 0$ can be converted to $\nu_{H=0}$ with expression (2) and the known g value[38] of MnF_2. All magnetic field values had to be multiplied by a factor $(1-\frac{1}{2}\alpha)$ as required by Eq. (2). The values of this factor were obtained by combining Griffel and Stout's[16] values of $\chi_\perp - \chi_{\text{II}}$ with $\chi_\perp$ from Bizette and Tsai.[21] Griffel and Stout give a percentage error of 1%. No experimental errors are given, however, by Bizette and Tsai.

The results of this calculation are shown for the temperature range 4 to 21°K in Fig. 4. Here $\nu(T)/\nu(0)$ is plotted, where the value $\nu(4.2\text{°K}) = 261.4$ kMc/sec is adopted as $\nu(0)$. This is correct within the experimental errors. The nuclear magnetic resonance (NMR) frequency[39] of F^{19} in MnF_2 is also shown in Fig. 4. It is noted that these points (indicated by squares) lie above the AFMR curve. If, however, $[\nu(T)/\nu(0)]_{\text{NMR}}^{1.45}$ is plotted instead (triangles), the points fall on the AFMR curve within the experimental errors. According to the calculation of Oguchi

$$[\nu(T)/\nu(0)]_{\text{AFMR}} = [M(T)/M(0)]^{1.45}.$$

(The exponent would be 1.5 instead of 1.45 from molecular field theory with complete correlation of adjacent spins.) Now if the hyperfine interaction constant of F^{19} in MnF_2 is independent of temperature, $[\nu(T)/\nu(0)]_{\text{NMR}}$ should measure the temperature dependence of the sublattice magnetization. Therefore one might expect

$$[\nu(T)/\nu(0)]_{\text{AFMR}} = [\nu(T)/\nu(0)]_{\text{NMR}}^{1.45}. \tag{26}$$

TABLE I. The temperature, frequency, and line width for observations of AFMR at zero applied magnetic field.

T (°K)	$\nu_{H=0}$ (kMc/sec)	$\Delta\nu$ (kMc/sec)
63.6±0.5	96	~10.6
62.3±0.8	117	~9.5
57.5±0.8	142	~8.5
57.5±0.6	146	~8.4
41.8±0.3	212.7	~2.0
24.7±0.3	247.2	~1.4

[38] $g = 2.00$ in the paramagnetic state [J. W. Stout and C. A. Hutchison, Jr. (private communication)].
[39] V. Jaccarino (to be published).

It is seen that the experimental results confirm such an expression (and hence a high degree of correlation of adjacent spins) very well. In the intermediate temperature region, the NMR data and the AFMR measurements show that a high degree of correlation between spins must still exist in this region. Rather surprisingly, Eq. (9) appears to hold approximately up to about 54°K.

In order to test the validity of Eq. (10a), $H(1-\alpha/2)$ was plotted against $T^2M(T/T_{AE})$. From the resulting straight line, the multiplicative constant a was determined to be 8.13×10^{-5} ($\pm8\%$). The error quoted here includes possible systematic errors. Using this value of a, $[M(T)/M_\infty]^{1.45}=0.9568-aT^2M(T/T_{AE})$ is shown *versus* $H(1-\frac{1}{2}\alpha)$ in Fig. 5. Since $(1-\frac{1}{2}\alpha)$ is close

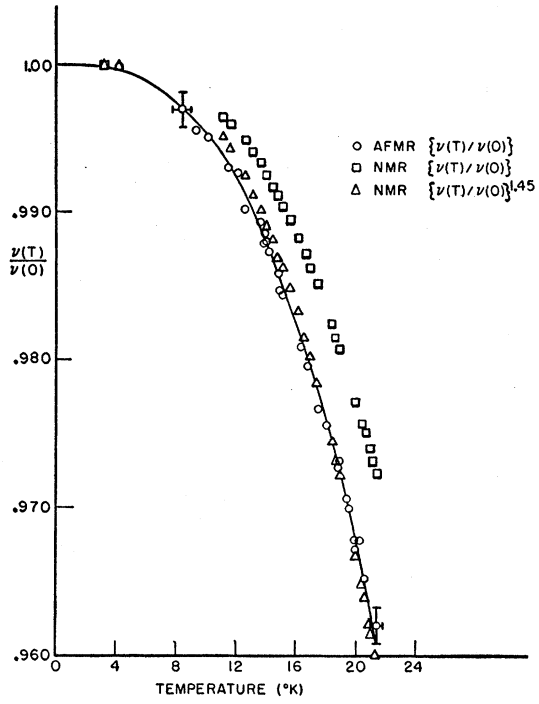

FIG. 4. Temperature dependence of $[\nu(T)/\nu(0)]_{AFMR}$, $[\nu(T)/\nu(0)]_{NMR}$ and $[\nu(T)/\nu(0)]_{NMR}^{1.45}$.

to unity over this temperature range (dropping to 0.93 at 22°K), errors due to uncertainties in $(1-\frac{1}{2}\alpha)$ are believed negligible up to 22°K. The straight line of Fig. 5 seems to verify the $T^2M(T/T_{AE})$ temperature dependence of the sublattice magnetization [Eq. (5)]. Equation (5), then, in conjunction with Eq. (9) is sufficiently good to determine $\nu(T)$ to within about 0.1% of its measured value in the temperature range 4 to 22°K. This would imply that spin wave theory can also predict the temperature dependence of the sublattice magnetization to about 0.1% of its value in this range. Furthermore, the value of $z|J|$ determined from Eq. (10b) and the multiplicative constant a agrees well with other determinations of $z|J|$ (see Table II). $z|J|$ can also be determined from Eq. (13) if the calculated[19]

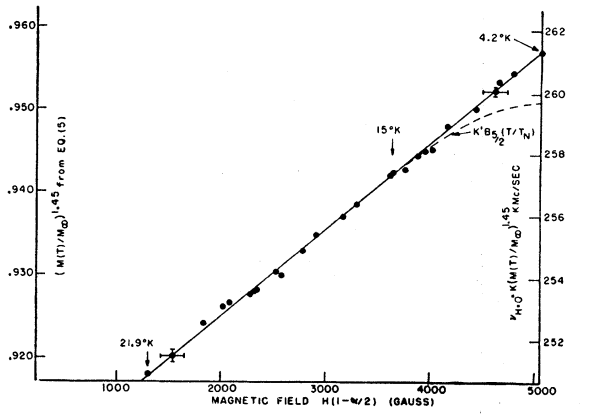

FIG. 5. Plot of $\nu_{H=0}(T)=[M(T)/M_\infty]^{1.45}$ *versus* $H(1-\frac{1}{2}\alpha)$ Typical experimental[37] errors are indicated. The original data of T *vs* H were converted by means of Eq. (5) to $[M(T)/M_\infty]^{1.45}$ to test the validity of Eq. (5). These are the same points as in Fig. 4, but replotted with different axes.

value of the anisotropy energy, E_A, is used. Alternatively, from Eq. (13) with the experimental value of $z|J|$ as determined from Eq. (10), the anisotropy energy is determined to be 5.0×10^6 ergs/cc.

It might be noted that above 15°K, the straight line can also be represented by the modified Brillouin function, Eq. (2) plus Eq. (4), with $K'=259.7$ kMc/sec. However, this function deviates from a straight line below about 15°K. The fact that the Brillouin function fits the experimental frequencies above 15°K actually implies that the magnetization falls off more slowly with temperature than the Brillouin function, since some degree of local order must still be present. Local order then would tend to reduce the previously mentioned[12] discrepancy between the AFMR and neutron scattering[15] results. It might be pointed out that Néel in 1932 predicted that because of fluctuations of the nearest neighbors the magnetization of the sublattices should be appreciably greater than that given by molecular field theory.[40]

The data represented in Figs. 4 and 5 are a composite from a number of runs taken under different conditions. Some points are actually a mean of three separate

TABLE II. Values of $z|J|$ for MnF_2 in the antiferromagnetic state.

Method by which $z\|J\|$ is obtained	$10^{15}\times z\|J\|$[a] (ergs)
AFMR: from $\nu(0)$, Eq. (13)	3.94 ± 0.03[b]
AFMR: from slope of $\nu(T)$, Eq. (10)	3.85 ± 0.15[b]
Susceptibility measurements ($\chi_\perp$)[c]	4.25
Specific heat measurements[d, e]	3.82
Molecular field theory[f]	3.20
Calculation including short-range order[g]	3.73

[a] J is equal to twice the exchange integral.
[b] Only experimental errors are shown here.
[c] H. Bizette and B. Tsai, reference 21.
[d] J. W. Stout and H. E. Adams, J. Am. Chem. Soc. **64**, 1535 (1942).
[e] Hofman, Pakin, Tauer, and Weiss, J. Phys. Chem. Solids **1**, 45 (1956).
[f] J. H. Van Vleck, reference 17: $z|J|=3kT_N/S(S+1)$.
[g] H. A. Brown and J. M. Luttinger, Phys. Rev. **100**, 685 (1955).

[40] L. Néel, Ann. Physik **28**, 1 (1932).

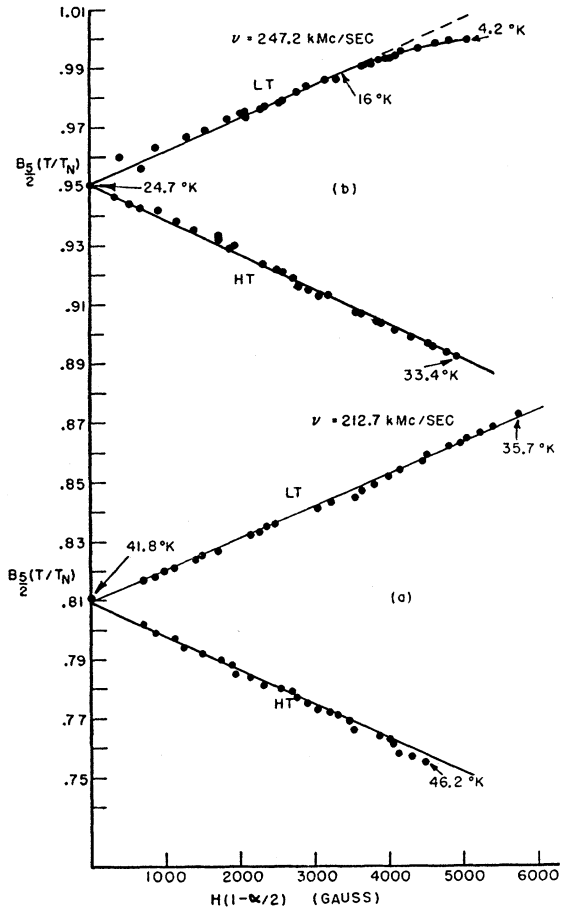

FIG. 6. Plot of $B_{5/2}(T/T_N)$ *versus* $H(1-\alpha/2)$. (a) $\nu=212.7$ kMc/sec, (b) $\nu=247.2$ kMc/sec. The original data of T *versus* H were converted to $B_{5/2}(T/T_N)$ *versus* H to test the validity of Eq. (4).

measurements. The error indicated on the graph represents the probable error of an individual measurement.

In Fig. 6 are plotted the AFMR experimental points on the assumption that Eqs. (2) and (4) are satisfied. Values of $B_{\frac{5}{2}}(T/T_N)$ are plotted *versus* $H(1-\frac{1}{2}\alpha)$. The two resonant modes, designated LT and HT,[41] were observed in each case at the given applied frequency. This mode of presentation of the data was used initially in order to show that $\nu(T)/\nu(0)$ was proportional to $B_{\frac{5}{2}}(T/T_N)$. As mentioned before, it now appears that this relationship is probably fortuitous. If, as an empirical relation, one assumes Eq. (4) to hold, then the data of Fig. 6 should appear as a pair of straight lines. Figure 6 shows the data to be well represented by the Brillouin function in the high-temperature region. However, some deviation is shown by the fact that the slopes of the HT and LT branches differ by about 12%. This difference might be accounted for by various effects such as shifts due to asymmetric line shape and shifts due to Eq. (22). By means of a least-squares analysis, the values for the intercepts of the HT and LT branches at a frequency of 212.7 kMc/sec were, respectively, $B(T/T_N)=0.810$ and $B(T/T_N)=0.8086$, and at $\nu=247.2$ kMc/sec the values were $B(T/T_N)=0.9527$ and $B(T/T_N)=0.9524$. This leads to a value of $\nu(0)=247.2/0.9525=259.5$ kMc/sec, to be compared with the better value of 261.4 kMc/sec derived from the magnetic field for resonance at 4.2°K and 247.2 kMc/sec.

It can be seen in Fig. 6(b) that the Brillouin function fails to describe the resonance frequency below about 15°K. The dotted line corresponds to the spin-wave results previously given in Fig. 5.

Finally, all measurements of $\nu_{H=0}$, together with data converted to $H=0$ from Eq. (2) with $g=2.00$, are given in Fig. 7. Here $\nu(T)$ is plotted *versus* T. For the solid curve, a value of $K'=261.4$ kMc/sec was used in Eq. (4). Figure 7 shows a slight tendency for points to be to the right of the curve given by Eq. (4). However, these deviations are all within experimental errors except below 15°K, where Eq. (4) does not hold.

Qualitative observations were made as various angles were changed. When the crystal was rotated at constant temperature and frequency with fixed mutually perpendicular dc and rf magnetic fields, the intensity of the absorption rapidly decreased as the symmetry axis was rotated away from the direction of the dc field. In addition, the magnetic field necessary for resonance increased. This increase in magnetic field was also observed as the dc magnetic field was rotated with the rf field and crystal fixed. These rotation experiments verified that the symmetry axis of the crystal coincided with the magnetic anisotropy axis, in agreement with other measurements.

Foner[13] has made AFMR measurements on MnF_2 by observing the HT branch, using large pulsed magnetic fields (of the order of 90 kgauss). At these high fields,

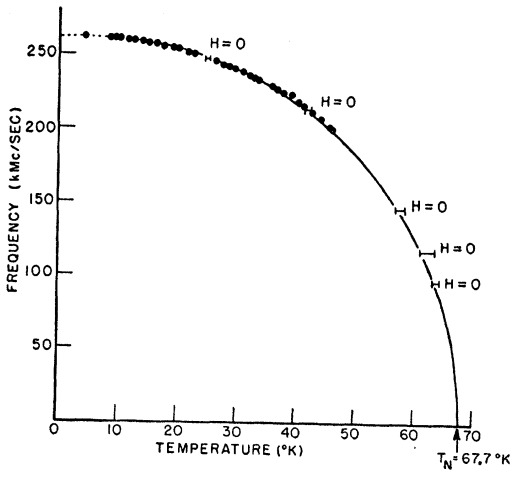

FIG. 7. $\nu_{H=0}(T)$ *versus* temperature. Circles represent experimental values of $\nu_{H\neq 0}(T)$ which were converted to $\nu_{H=0}(T)$ by means of Eq. (2). The points below 21°K have been shown in Fig. 4 on an expanded scale.

[41] These correspond to ω_3 and ω_2, respectively, in the notation of Keffer and Kittel.

possible errors due to crystal misalignments become more serious. Also, uncertainties in the $(1-\frac{1}{2}\alpha)$ factor begin to be important. The present measurements should be considerably more accurate than Foner's, and give resonance frequencies about 4% lower.

A comparison of measurements on MnF_2 with those on $CuCl_2 \cdot 2H_2O$ [9] indicates many similarities despite the fact that the copper chloride lattice has rhombic symmetry and also a more complicated magnetic lattice structure than MnF_2. Analysis of proton NMR measurements[42] in copper chloride indicate a slower drop in magnetization with increasing temperature than the AFMR measurements do, as is also the case for MnF_2 (this has been explained for MnF_2 at low temperatures by Oguchi's calculation).

VI. LINE WIDTHS

The AFMR line shape at 4.2°K is shown in Fig. 8 for a slab of about 0.0045-in. thickness. This curve represents the average values of four separate runs. Its shape has been approximately matched (dashed line) by choosing appropriate values of the constants in Eqs. (22) and (23), consistent with about 8% transmission at the peak of the resonance line. The value of A/δ was taken to be 2 and $\delta=150$ gauss. These values are consistent with the theoretical estimate of $A=320$ gauss [Sec. IV, Eq. (19)]. (The dielectric constant[43] was taken to be 6.7.)

The temperature dependence of the line width $\Delta\nu=2\delta$ *versus* T/T_N is shown in Fig. 9, where the indicated errors include errors due to uncertainties in estimating the line widths because of the asymmetric line shape. On the same graph are also shown the AFMR line

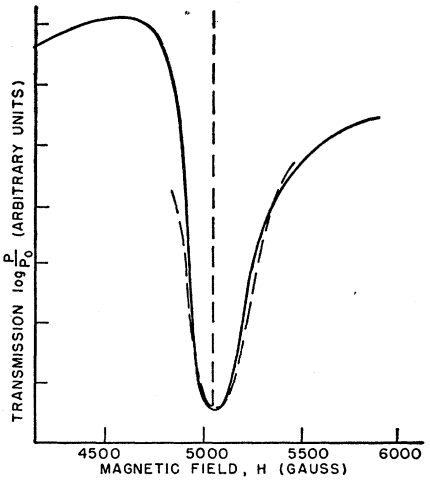

FIG. 8. AFMR line shape. Shown for slab (B) of 0.0045-in. thickness at 4.2°K. The solid curve represents the average of four separate measurements. The dashed line is the theoretical curve based on Eqs. (22) and (23), assuming $\Delta\nu\simeq 300$ gauss, $A/\delta=2$, and $\delta=150$ gauss.

[42] N. J. Poulis and G. E. G. Hardeman, Physica **19**, 391 (1953).
[43] We are grateful to Mr. W. B. Westphal and also to Mr. H. M. Altschuler for measuring the dielectric constant of MnF_2.

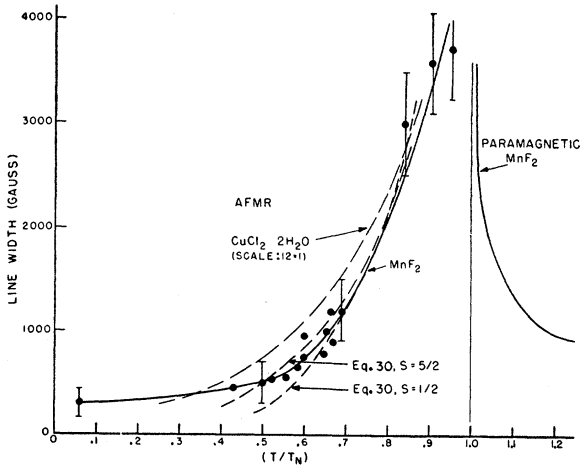

FIG. 9. AFMR line widths. The line widths of MnF_2 are shown by the solid line. The line-width curve for $CuCl_2 \cdot 2H_2O$ was multiplied by a factor of 12 to facilitate intercomparison. Equation (30), normalized at $T/T_N=0.8$, is plotted for spins $\frac{5}{2}$ and $\frac{1}{2}$.

widths of copper chloride,[44] for the corresponding LT resonant mode, normalized so that the line widths coincide at low temperatures. It seems that the two antiferromagnetic materials have a similar temperature dependence. This seems to suggest that the line-broadening mechanism in both materials is of a similar nature. Also the fractional line widths for both materials $(\Delta\nu/\nu)$ are of the same order of magnitude $(\sim 3\times 10^{-3})$, where ν is the resonance frequency. The temperature dependence of the line width of MnF_2 in the paramagnetic[45] region $(T/T_N>1)$ is also shown in Fig. 9.

Theory of Line Width

A calculation of AFMR line width from a particular model was made by Townes.[46] This model assumes that there are fluctuations[47] of the effective molecular field at the site of an individual spin.

Although this model has the limitation that it uses molecular field theory and especially that it neglects spin correlations, it will be briefly outlined here since it qualitatively predicts the observed line width and its temperature dependence.

The model assumes that each individual magnetic moment is surrounded by n spins, of spin $\frac{1}{2}$ each (e.g., in MnF_2 at any particular lattice site of Mn^{++}, replace the 8 neighboring spins of $\frac{5}{2}$ by 40 spins of $\frac{1}{2}$ each). The probability, P_m, that m spins are pointing in a specified direction is given by

$$P_m=\frac{n!e^{mx}}{(1+e^x)(n-m)!m!}. \tag{27}$$

[44] H. J. Gerritsen and M. Garber, Physica **22**, 213 (1956).
[45] C. A. Hutchison and J. W. Stout (private communication).
[46] C. H. Townes (private communication).
[47] A similar calculation was made by Néel, see reference 40. However, Néel calculated the susceptibility and magnetization and not the line width.

From this one may compute $\bar{m}$ and $\langle m^2\rangle_{\text{Av}}$ and hence

$$(\Delta m)^2=\langle m^2\rangle_{\text{Av}}-\bar{m}^2,$$

where

$$\bar{m}=\frac{ne^x}{1+e^x} \quad \text{and} \quad \langle m^2\rangle_{\text{Av}}=\frac{ne^x(1+ne^x)}{(1+e^x)^2}. \tag{28}$$

Here x is a function of temperature and the total effective magnetic field. From molecular field theory, $\bar{m}$ can be related to the Brillouin function and to $\nu(T)$. The following expression for the line width is then obtained:

$$\Delta\nu_p=\frac{\nu(0)}{\sqrt{n}}\left[1-\left(\frac{\nu(T)}{\nu(0)}\right)^2\right]^{\frac{1}{2}}. \tag{29}$$

Exchange narrows the line[48] so that $\Delta\nu\simeq\langle\Delta\nu_p\rangle^2/\nu_{\text{ex}}$, where $\Delta\nu_p$ is the line width expected in the absence of exchange forces and ν_{ex} is the exchange frequency. Assuming for simplicity that $\nu(T)/\nu(0)\simeq B_S(T/T_N)$, the final expression for the line width is as follows:

$$\Delta H=\frac{2H_A(0)}{n}\left\{\frac{1}{B_S(T/T_N)}-B_S(T/T_N)\right\}. \tag{30}$$

A comparison of experimental results at intermediate temperatures with this expression may be made. For MnF_2, at $T/T_N=0.8$ ($T=54°K$), $(\Delta H)_{\text{expt}}=2100$ gauss and a value of $n=8$ is obtained (40 would be expected from eight neighbors of spin $\frac{5}{2}$ if no correlation is assumed). Similarly, for $CuCl_2\cdot 2H_2O$ at $T/T_N=0.83$, ($T=3.6°K$) and with $H_A(0)\simeq 80$ gauss, $(\Delta H)_{\text{expt}}=220$ gauss, a value of the order of unity is obtained for n, whereas eight would be expected. The temperature dependence of expression (30) (normalized at $T/T_N=0.8$) is plotted in Fig. 9 for spins $\frac{5}{2}$ and $\frac{1}{2}$. This shows good qualitative agreement between the experimental results and Eq. (30).

This type of broadening will produce a line width for the fluorine nuclear resonance of approximately γ_e/γ_N ($\simeq 650$) times smaller than the AFMR line width, or $\frac{1}{2}$ gauss at 4°K. Nuclear line widths of approximately 14 gauss have been observed[22] and this can be ascribed primarily to nuclear dipole-dipole broadening.

Analysis of Crystals

Two single crystals of MnF_2, each obtained from a different source[49,50] and grown under quite different physical conditions were used in this experiment. One major difference was that one crystal (designated as A) was grown in a fluorine atmosphere[51] and the other in a nitrogen atmosphere. The measurements reported previously[12] were made entirely on slabs cut from the single crystal (A) which had been grown by Stout. Subsequently, a second crystal (designated as B) was obtained and intercomparisons of the frequency and line width were made.

Inasmuch as the resonance frequency depends critically on the orientation of the sample and might also depend critically on strains and microscopic misalignments, it was thought important to see whether the line width and frequency might vary from sample to sample.

AFMR measurements were made at a frequency of 212.7 kMc/sec on slabs of about equal thickness and oriented with the c axis parallel to the external field. The results indicated no apparent shifts of the absorption line either in temperature or magnetic field. Also, at temperatures above 33°K the line widths for slabs cut from crystal specimen A or from B were approximately equal. These results were of particular interest since some slight crystallographic differences were detected between A and B.

Examination with a polarizing microscope established that crystal A was essentially uniaxial. However, crystal B was found to be slightly biaxial.[52] The angle V between the acute bisectrix[53] and either optic axis was measured to be 1.3° for the bulk crystal specimen B. Measurements on different slabs cut from crystal B gave values for the angle V which varied from about 1° to about 3°. This might be evidence for crystal strains or some other type of crystal imperfection.

The data at the lowest temperatures were taken only with crystal B. However, since at higher temperatures the line width was approximately the same for both samples, it would appear that at least this type and degree of imperfection plays no significant role in the line-width problem at these higher temperatures. The residual line width in crystal B at 4°K presumably arises from a nonthermal origin. Further investigations of the origin of this anomalous residual line width at 4°K might include measurements of AFMR line widths on a specially annealed crystal specimen, or perhaps on crystals which have a large degree of imperfection.

VII. SUBSIDIARY MODES

Under certain experimental conditions a subsidiary transmission minimum was observed even though the sample was supposedly placed in its usual position across the guide. This particular extra minimum was always considerably weaker than the main mode and was separated from it by about 3000 gauss [see Fig. 10(c)]. It was observed in only one sample, which was misaligned crystallographically by about 5°. Also, this peak

[48] P. W. Anderson and P. R. Weiss, Revs. Modern Phys. **25**, 269 (1953); P. W. Anderson, J. Phys. Soc. Japan **9**, 316 (1954).

[49] We are greatly indebted to Professor J. W. Stout for providing specimens of MnF_2.

[50] We are greatly indebted to Dr. B. V. Rollin and Dr. D. A. Jones for providing specimens of MnF_2 grown by Dr. Jones.

[51] M. Griffel and J. W. Stout, J. Am. Chem. Soc. **72**, 4351 (1950).

[52] Normally uniaxial crystals or minerals can be biaxial. See A. F. Rogers and P. F. Kerr, *Optical Mineralogy* (McGraw Hill Book Company, New York, 1942). We are indebted to Professor P. F. Kerr for assistance with these measurements.

[53] E. E. Wahlstrom, *Optical Crystallography* (John Wiley & Sons, Inc., New York, 1956).

occurs on the side of the main peak, where destructive interference is probably effective in altering the transmission; such effects could result in extra peaks. Because of possible misalignment and interference effects, it could not be decided whether this extra mode was significant or not.

Various other samples were then placed in other positions, particularly against the wall of the wave guide. A number of new modes were observed, examples of which are given in Figs. 10(d) and 10(e). These commonly were quite strong and the central peaks might often be missing or displaced. These modes showed an extreme separation in field of about 2700 gauss.

Also, curves were taken with the sample in its normal position, but with a TE_{03} mode transducer and filter in place. A typical curve is shown in Fig. 10(g). However, extra and finer structure appeared with this arrangement, and this structure was sensitive to supposedly immaterial adjustments, such as the crystal detector tuning plunger. This arrangement, therefore, did not give any important clues as to the origin of these modes.

Although these subsidiary modes seem similar to the magnetostatic modes discovered previously,[54,55] in ferrimagnetic resonance, the splittings of 4000 gauss [or 2700 gauss if Fig. 10(c) is discarded] are much too large

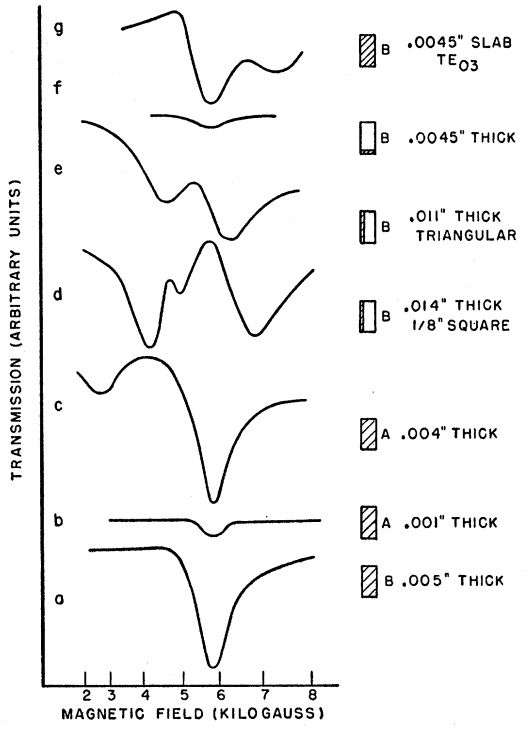

FIG. 10. Typical absorption contours are shown for various samples and sample orientations at about the same temperature (37°K). Except for case (g), microwave propagation was in the TE_{01} mode.

[54] J. F. Dillon, Jr., Bull. Am. Phys. Soc. Ser. II, **1**, 125 (1956).
[55] R. L. White and I. H. Solt, Jr., Phys. Rev. **104**, 56 (1956).

to be explained by this effect.[56] It can be shown either from Eq. (33) of Keffer and Kittel[5] or from an extension of the method of Walker[57] that the extreme magnetic field splitting for ellipsoids of revolution is

$$\Delta H_{\max}=\frac{N_T'-N_T''}{H_E}M(T)(2H_EH_A)^{\frac{1}{2}}, \qquad (31)$$

where N_T' and N_T'' are the two extreme transverse demagnetizing coefficients and can be taken from Walker's Fig. 4.[58] It should be noted that the situation in a ferrimagnetic material is rather different from that in an antiferromagnetic material where $M_z=0$ and N_z is not effective in increasing the magnetic field splittings (for ferrimagnetic ellipsoids N_z causes an increase in splitting by a factor of three, *viz.*, from $0\rightarrow 2\pi M$ to $-4\pi M\rightarrow 2\pi M$).

Certainly the extreme limits for N are $\pm 4\pi$. Numerical evaluation then gives $\Delta H_{\max}=2.8$ kilogauss. However, for regular ellipsoids with $M_z=0$, $N_T'=2\pi$ and $N_T''=0$, one obtains $\Delta H_{\max}=0.7$ kilogauss.

It should be pointed out that the above results were derived for ellipsoids whose effective size is small compared to a wavelength. However, the basic situation is not qualitatively altered when propagation effects can occur (see, e.g., reference 37). Surface divergences in the direction of propagation are replaced by volume divergences, but these divergences are of about the same size. Therefore, the effective demagnetizing factors and field splittings remain about the same.

The difference between the observed 4000 (or possibly 2700) kilogauss and the predicted 700 gauss is considerable. Dispersion effects are unlikely to cause a sufficient increase in the predicted 700-gauss splitting. It would seem more likely that reflection and interference effects are responsible for at least some of the observed modes. However, no detailed explanation can be given.

It is strongly believed that the peak of Figs. 10(a) and 10(b) is the correct uniform mode of precession. In any case, the splittings of the subsidiary modes are small relative to $\nu(T)$ and would, therefore, make only minor quantitative readjustments of the results of the other sections necessary if this identification is incorrect. None of the general conclusions would be altered.

VIII. CONCLUSIONS

This paper reports on AFMR measurements on single crystals of MnF_2. Measurements of the resonance frequency, $\nu(T)$, were made from 96 kMc/sec to 247.2 kMc/sec and in the temperature range from 4°K to 64°K. The resonance frequency $\nu(0)$ was determined to

[56] We are indebted to Dr. H. Suhl and Dr. R. L. White for interesting communications on the magnetostatic mode problem.
[57] L. R. Walker, Phys. Rev. **105**, 390 (1957).
[58] Equations (7), (9), (10), and (18) of Walker's paper hold good if κ and ν are redefined as $\kappa=4\pi\gamma^2MH_A(\Delta_1+\Delta_2)$ and $\nu=4\pi\gamma^2MH_A(\Delta_1-\Delta_2)$, where $1/\Delta_{1,2}=(\omega\mp\gamma H)^2-\gamma^2(H_A^2+2H_EH_A)$.

be 261.4±1.5 kMc/sec. Measurements of $\nu(T)$ at other temperatures are shown in Figs. 4 and 7. The shape of the resonance curve was found to be asymmetric. The line width and its dependence on temperature were measured, the full line width at the half intensity point of μ_2 was found to be 300±140 gauss at 4°K. From the resonance relations and the measured value of $\nu(0)$, the anisotropy energy was determined to be 5.0×10^6 ergs/cc. Also, from Oguchi's theoretical analysis of the anisotropy energy and the above value of $\nu(0)$, the quantity $z|J|$ is inferred to be 3.94×10^{-15} erg, in good agreement with other determinations (Table II).

The results can be understood on the basis of the general resonance relations $[\omega/\gamma=(2H_EH_A)^{\frac{1}{2}}\pm(1-\frac{1}{2}\alpha)H]$ derived by Nagamiya and Keffer and Kittel. In the low-temperature region, 4°K to 22°K, the AFMR results are consistent with spin-wave calculations of the temperature dependence of the sublattice magnetization and of the dependence of the anisotropy energy on the magnetization. In fact, the spin-wave theory predicts the AFMR frequency to about 0.1% of its measured value, which implies that it can also predict the magnetization to about the same accuracy at any temperature in this low-temperature range.

These results show that there is almost complete correlation of neighboring electron spins in the low-temperature region and that a high degree of correlation continues to much higher temperatures. Because of this correlation, the anisotropy energy and hence the AFMR frequency would not be expected to be directly proportional to the magnetization. Indeed, other measurements of the magnetization fall above the curve of AFMR frequencies *versus* temperature. It would seem, therefore, that the close correspondence of AFMR frequencies and the Brillouin function may be accidental.

The observed asymmetric line shape can be qualitatively accounted for by the contribution made to the imaginary part of the propagation constant by the real part of the susceptibility. The line width can be qualitatively explained by a simplified thermal fluctuation model, even though it neglects electron spin correlations. Finally, the results of AFMR measurements on two crystals, which were grown under different conditions, indicated no difference in resonance frequency or line width.

IX. ACKNOWLEDGMENTS

We wish to take this opportunity to express our great appreciation to Professor C. H. Townes for his active interest and aid throughout the course of this research. We wish to thank Professor P. F. Kerr for his generous help with the crystallographic analysis and x-ray measurements, and Professor T. I. Taylor for the use of some of his equipment. We are grateful for the assistance of the staff of the Columbia Radiation Laboratory, in particular Mr. M. J. Bernstein and Mr. C. O. Dechert. We have benefitted from helpful discussions with and communications from Professor B. Bleaney, Professor R. S. Halford, Dr. V. Jaccarino, Dr. H. J. Gerritsen, and especially Professor F. Keffer. We also wish to thank Dr. T. Oguchi and Dr. V. Jaccarino for sending us their manuscripts prior to publication.